

THE EXOPLANET ECCENTRICITY DISTRIBUTION FROM KEPLER PLANET CANDIDATES

STEPHEN R. KANE, DAVID R. CIARDI, DAWN M. GELINO, KASPAR VON BRAUN

NASA Exoplanet Science Institute, Caltech, MS 100-22, 770 South Wilson Avenue, Pasadena, CA 91125, USA

Submitted for publication in the Astrophysical Journal Letters

ABSTRACT

The eccentricity distribution of exoplanets is known from radial velocity surveys to be divergent from circular orbits beyond 0.1 AU. This is particularly the case for large planets where the radial velocity technique is most sensitive. The eccentricity of planetary orbits can have a large effect on the transit probability and subsequently the planet yield of transit surveys. The Kepler mission is the first transit survey that probes deep enough into period-space to allow this effect to be seen via the variation in transit durations. We use the Kepler planet candidates to show that the eccentricity distribution matches that found from radial velocity surveys to a high degree of confidence. We further show that the mean eccentricity of the Kepler candidates decreases with decreasing planet size indicating that smaller planets are preferentially found in low-eccentricity orbits.

Subject headings: planetary systems – techniques: photometric – techniques: radial velocities

1. INTRODUCTION

Planets discovered using the radial velocity method have dominated the total exoplanet count until recent years during which the transit method has also greatly contributed to this number. The time baseline for radial velocity surveys has allowed the detection of a far more diverse range of orbital geometries than achievable by ground-based transit surveys. However, the Kepler mission has allowed the transit method to probe deep into period-space such that comparisons with the radial velocity distributions can begin to be made.

One particular aspect of orbital geometry which is able to be investigated at longer periods is that of orbital eccentricity. It has been shown for the radial velocity planets that orbits can diverge significantly from the circular case beyond semi-major axis of ~ 0.1 AU (Butler et al. 2006), although there may be small observational biases which skew this distribution (Shen & Turner 2008). This has led to numerous attempts to explain the eccentricity in the context of planet formation and orbital stability (Ford & Rasio 2008; Malmberg & Davies 2008; Matsumura et al. 2008; Jurić & Tremaine 2008; Wang & Ford 2011) and the influence of tidal circularization (Pont et al. 2011).

It has additionally been shown how this eccentricity distribution effects transit probabilities (Kane & von Braun 2008, 2009) and the subsequent impact on the results of transit surveys (Burke 2008). This impact is negligible for the ground-based surveys since they are only sensitive to giant planets in short-period orbits. However, the Kepler mission is expected to be impacted by this distribution since it probes out to much longer periods without the disadvantage of a window function which affects observations from the ground (von Braun et al. 2009). A comparison of the Kepler results in the context of eccentricity and transit durations with the radial velocity distribution has been suggested by Ford et al. (2008) and Zakamska et al. (2011), but initial planet candidate releases by the Kepler project do not provide enough period sensitivity

(Borucki et al. 2011a,b). The most recent release of Kepler planet candidates by Batalha et al. (2012) increases the total number of candidates to more than 2,300 and the period space probed to beyond 560 days.

Here we present a study of the eccentricity distribution of planets discovered with the radial velocity method and compare this with the complete list of Kepler planet candidates. In both cases, we calculate transit durations for circular orbits and compare these values with either calculated or measured eccentric transit durations. Our results show that the measured transit durations from the Kepler candidates match the expected transit durations from the radial velocity. We estimate the impact parameter distribution for the Kepler candidates. We further show that the mean eccentricity of the Kepler candidates decreases with decreasing planet size which supports the view that smaller planets tend to be found in multiple systems in near-circular orbits.

2. ECCENTRICITY AND TRANSIT DURATION

A concise description of exoplanetary transit modeling and associated parameters is presented elsewhere (Mandel & Agol 2002; Seager & Mallén-Ornelas 2002). Here we concentrate on the relevant details to this analysis; that of the transit duration and the effects of eccentricity. The transit duration for a circular orbit is given by

$$t_{\text{circ}} = \frac{P}{\pi} \arcsin \left(\frac{\sqrt{(R_{\star} + R_p)^2 - a^2 \cos^2 i}}{a} \right) \quad (1)$$

where P is the orbital period, a is the semi-major axis, i is the orbital inclination, and R_{\star} and R_p are the stellar and planetary radii respectively. The impact parameter of a transit is given by

$$b \equiv \frac{a}{R_{\star}} \cos i \quad (2)$$

and is defined as the projected separation of the planet and star centers at the point of mid-transit.

For an eccentric orbit, the star–planet separation r is time-dependent and is given by

$$r = \frac{a(1 - e^2)}{1 + e \cos f} \quad (3)$$

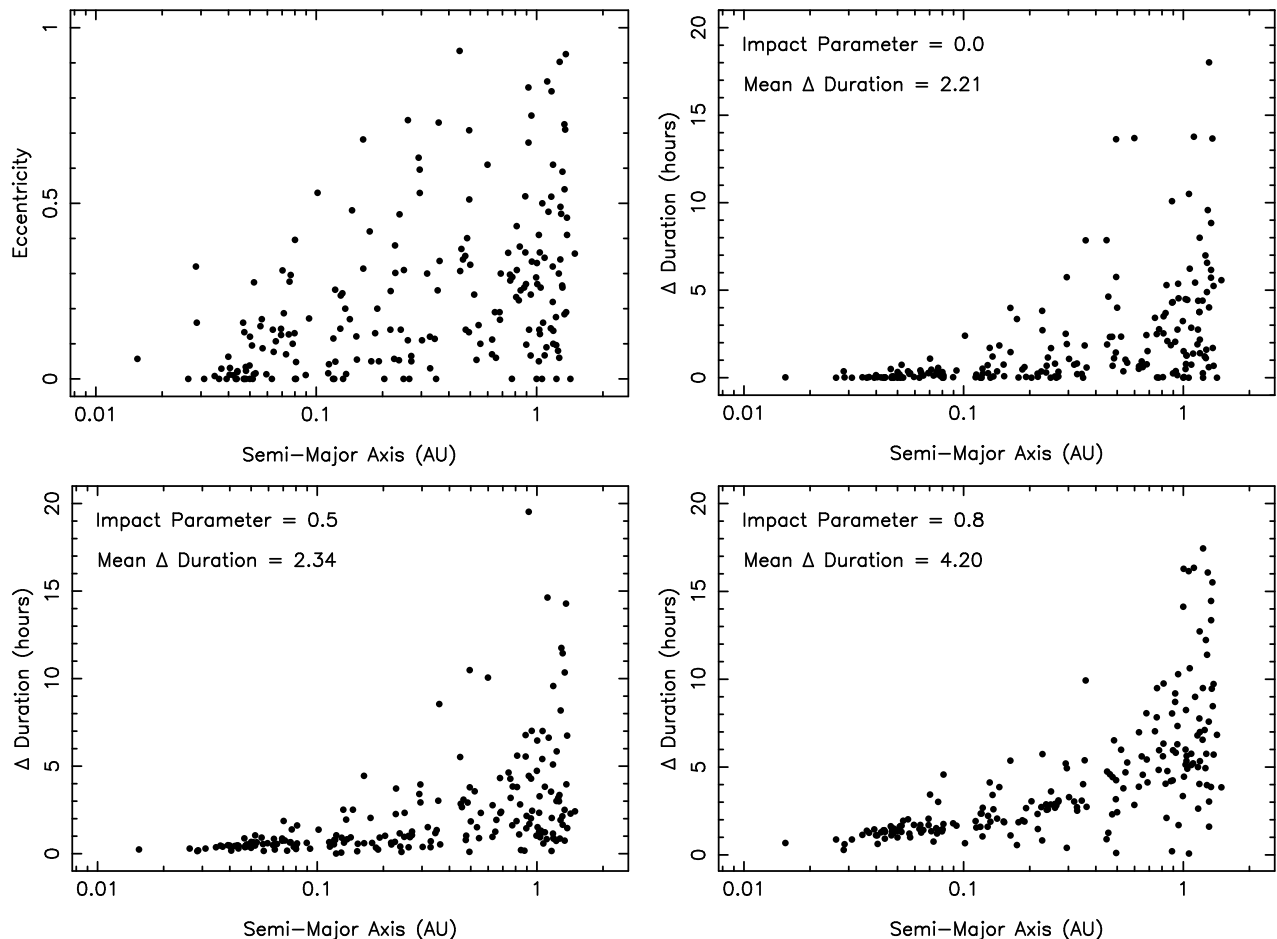


FIG. 1.— The eccentricity distribution of the known radial velocity planets (top-left) and the calculated transit duration difference (circular vs eccentric) for impact parameters of 0.0 (top-right), 0.5 (bottom-left), and 0.8 (bottom-right).

where e is the orbital eccentricity and f is the true anomaly. Thus we can replace a in the above equations with r to more accurately represent the instantaneous distance of the planet from the star. Additionally, Burke (2008) describes a scaling factor which can be used to calculate the transit duration for an eccentric orbit as follows

$$\frac{t_{\text{ecc}}}{t_{\text{circ}}} = \frac{\sqrt{1-e^2}}{1 + e \cos(\omega - 90^\circ)} \quad (4)$$

where ω is the periastron argument of the orbit.

3. RADIAL VELOCITY ECCENTRICITY DISTRIBUTION

We first investigate the eccentricity distribution of the planets which were discovered using the radial velocity technique and the subsequent impact on the predicted transit duration. The Exoplanet Data Explorer (EDE)¹ stores information only for those planets which have complete orbital solutions and thus are well suited to this study (Wright et al. 2011). The data extracted from the EDE are current as of 2012 February 24 and include 204 planets after the following criteria are applied: $\log g > 3.5$ to exclude giant stars and $a < 1.5$ AU to produce a sample which covers the same region in parameter space as the Kepler candidates.

¹ <http://exoplanets.org/>

To calculate the transit duration, one needs an estimate of the planetary radius. For planets which are not known to transit, we approximate the planetary radius using the simple model described by Kane & Gelino (2012) based on the mass of the planet. In order to estimate the radius of the host star, we use the following relation related to the surface gravity

$$\log g = \log \left(\frac{M_\star}{M_\odot} \right) - 2 \log \left(\frac{R_\star}{R_\odot} \right) + \log g_\odot \quad (5)$$

where $\log g_\odot = 4.4374$ (Smalley 2005). Using the equations of Section 2 and the measured orbital parameters, we calculate the transit duration for both the circular and eccentric cases. We then take the absolute value of the difference between the two durations as a diagnostic of the eccentricity distribution.

Figure 1 shows the result of these calculated distributions. The top-left figure plots the eccentricity distribution of the radial velocity planets as a function of the semi-major axis. The distribution begins to significantly diverge from a pure circular model beyond 0.04 AU and by 0.1 AU has an eccentricity range of 0.0–0.5. This distribution is widely attributed to tidal damping of the orbits after the disk has dissipated. According to Goldreich & Soter (1966), the timescale for orbital circularization is $\propto a^{6.5}$ and $\propto M_\star^{-1.5}$ where M_\star is the stellar mass. Note therefore that the two planets inside of

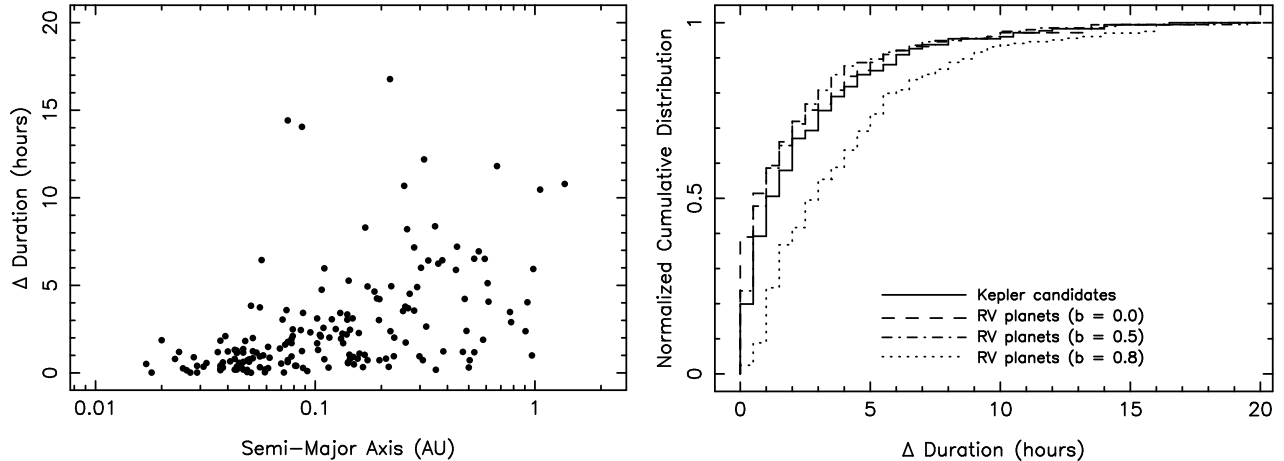


FIG. 2.— The calculated transit duration difference (circular vs measured) for the Kepler candidates (left). The cumulative histograms for the Kepler candidates and the three radial velocity planets shown in Figure 1 shows a close match between the distributions, quantified by the K-S test described in Section 4.

0.04 AU which have $e > 0.1$ are GJ 436b and GJ 581e, both of which have M dwarf host stars.

The other three panels in Figure 1 show the calculated duration difference represented by Δ Duration (i.e., Δ Duration = $|t_{\text{circ}} - t_{\text{ecc}}|$). The t_{ecc} value uses the measured orbital parameters for each case and so Δ Duration represents the divergence expected from the circular model. The top-right panel assumes edge-on orbits ($i = 90^\circ$) for both the circular and eccentric cases. The actual inclination could vary slightly from this however within the range allowed by Equation 2. The small range of allowed angles for a transit to occur means that a uniform distribution of i values maps to a uniform distribution of b values. We show the effect of increasing the impact parameter of the transits for $b = 0.5$ and $b = 0.8$. The mean of the Δ Duration is not significantly changed except for relatively high values of b . We evaluate the significance of this distribution in the following section.

4. ANALYSIS OF KEPLER TRANSIT DURATIONS

The release of more than 2,300 Kepler candidates is described in detail by Batalha et al. (2012). The appendix table, which contains the characteristics of the Kepler candidates, was extracted from the NASA Exoplanet Archive². We perform a similar calculation for Δ Duration as described in the previous section. However, this time we calculate the difference between t_{circ} and the duration measurement provided by the candidates table, t_{kepler} . We do not use the provided b values since these are based on a circular orbit assumption from the measured transit duration and the stellar radii. We thus make no assumption on the value of b . We do exclude those candidates for which $R_\star < 0.7R_\odot$ to remove the candidates for which the uncertainty in the stellar radius determination adds significantly to the scatter. We also only include candidates for which $R_p > 8R_\oplus$ to limit the sample to giant planets, similar to the radial velocity sample. This results in 176 candidates being selected. The calculations for these candidates are shown plotted in Figure 2.

To compare this distribution to those described in Sec-

TABLE 1
MINIMUM ECCENTRICITIES FOR SELECTED CANDIDATES.

KOI	Period (days)	t_{kepler} (hours)	Δ Duration (hours)	e_{min}
44.01	66.47	19.74	12.2	0.74
211.01	372.11	4.81	10.5	0.82
625.01	38.14	4.24	10.7	0.85
682.01	562.14	9.49	10.8	0.64
1230.01	165.72	27.26	11.8	0.34
1894.01	5.29	8.80	14.4	0.75
2133.01	6.25	11.26	14.1	0.67
2481.01	33.85	14.95	16.8	0.64

tion 3 we perform a Kolmogorov-Smirnov (K-S) test to assess the statistical significance of their similarities. In each case, we binned the data by Δ Duration into 40 equal bins of 0.5. Figure 2 shows the normalized cumulative histograms for each of these distributions. The three K-S tests compared the Kepler candidates to the radial velocity planets with $b = 0.0$ (Test 1), $b = 0.5$ (Test 2), and $b = 0.8$ (Test 3). Test 1 produced a K-S statistic of $D = 0.05$ which indicates a 100% probability that these are drawn from the same sample. Test 2 produced a similar result of $D = 0.075$, also a probability of 100%. Test 3 resulted in $D = 0.2$ which is equivalent to a probability of 36%. This quantitatively shows the differences one can see in the histograms in Figure 2 where the $b = 0.0$ and $b = 0.5$ cases are almost indistinguishable from the Kepler candidates whereas the $b = 0.8$ case departs from the distribution. As previously mentioned, the small angle of possible inclinations for transits results in a uniform distribution of impact parameters with a mean of $b = 0.5$. Clearly the distributions of transit durations discrepancies matches between the radial velocity planets and the Kepler candidates for the samples studied. This indicates that the observed eccentricity distribution is indeed been revealed by the Kepler mission as expected.

Finally, we investigate a sample of the outliers with particularly large deviations from the circular model (Δ Duration > 10 hours). These candidates are shown in Table 1. There is a degeneracy between the eccentricity and periastron argument that could produce the ob-

² <http://exoplanetarchive.ipac.caltech.edu/>

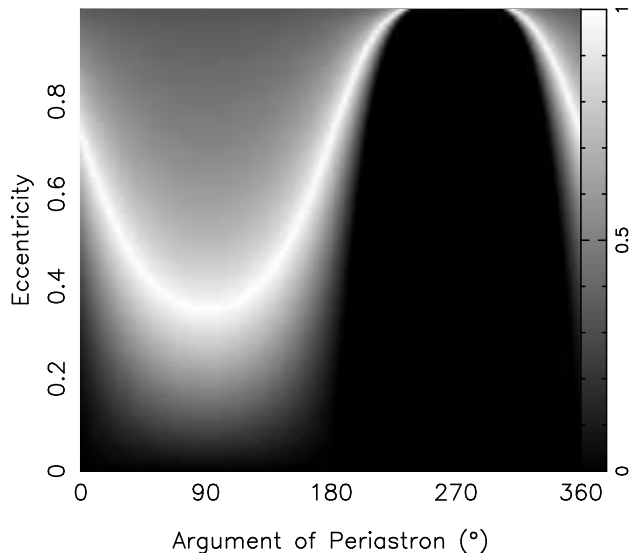


FIG. 3.— An intensity map for KOI 1230.01 which shows the result of dividing Δ Duration using t_{kepler} by Δ Duration using t_{ecc} . Thus, a value of 1 (peak intensity) corresponds to the best solution.

served duration discrepancy. In order to determine possible values for these two parameters, we calculate a new Δ Duration using a grid of e and ω values. The Δ Duration determination using t_{kepler} (see Figure 2) is then divided by this new value. In other words, we calculate $|t_{\text{circ}} - t_{\text{kepler}}| / |t_{\text{circ}} - t_{\text{ecc}}|$. Thus locations of the parameter space where this division is approximately equal to 1 are possible solutions. An example of this is represented in Figure 3 where we present these results as an intensity map for KOI 1230.01. In order to be compatible with the Kepler measured duration, the eccentricity of the planet must be at least 0.34. This process is repeated for each of the candidates in Table 1 in which we report the minimum required eccentricity e_{min} for each candidate. It is worth noting however that these minimum eccentricities are not hard limits but rather are distributions, as seen by the gray-scale in Figure 3. The uncertainty on these values depend highly upon the various uncertainties in the measured values of the Kepler candidates catalogue including the inclination of the orbit. For example, the stellar radius of KOI 2481 would need to be $\sim 45\%$ of the catalogue value in order for the duration discrepancy to be reduced to zero.

5. PLANET SIZE CORRELATION

It was mentioned in Section 4 that the analysis of the Kepler objects was conducted by only including those candidates for which $R_p > 8R_{\oplus}$. Here we perform a separate study by repeating the calculations of Δ Duration for the Kepler candidates for a range of planetary radii. We allow the candidate sample to include all radii larger than $1R_{\oplus}$ to $8R_{\oplus}$ and calculate the mean of the Δ Duration distribution in each case. The results of this are shown plotted in Figure 4.

An interpretation of this figure is that the eccentricity distribution of exoplanets remains relatively flat until we probe below planets the size of Neptune. At that point the eccentricity distribution of the orbits becomes rapidly and significantly more circular. One aspect of the Kepler candidate sample which may influence this result is that they are dominated by planets at smaller semi-major

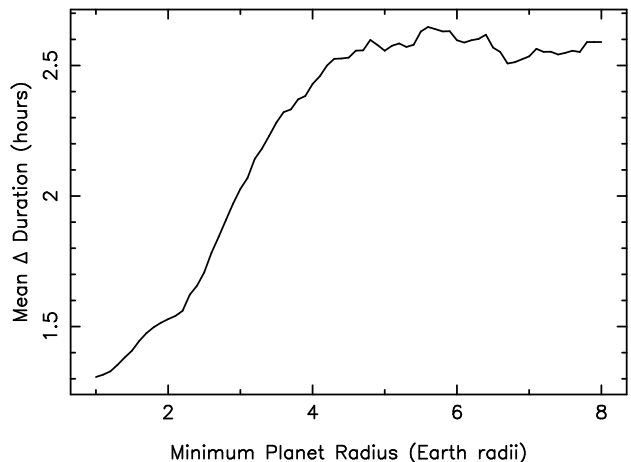


FIG. 4.— The mean Δ Duration for the Kepler candidates as a function of minimum planetary radius being included in the sample.

axes since these have much larger transit probabilities. As indicated by Lissauer et al. (2011) and Lissauer et al. (2012), multi-planet systems comprise a large proportion of the total Kepler candidate sample and these systems in particular are less prone to be false-positives. The findings that planet occurrence increase with decreasing planet mass (see Howard et al. (2010) for example) then suggests that smaller planets find stable architectures in systems with circular orbits and without large planets in eccentric orbits. This lends credence to the instability and capture scenarios which both explain the presence of eccentric giant planets and the absence of terrestrial planets.

One cause for the correlation shown in Figure 4 would be if there was a similar correlation of planetary radii with semi-major axis present in the Kepler sample. This would mean that smaller planets in closer orbits would be more likely to have had their orbits circularized leading to a biased sample. Such a radius/distance correlation is weak however with large planets being almost as uniformly sampled in semi-major axis space as the smaller planets. Thus this cannot be the cause of the observed radius/eccentricity correlation.

6. DISCUSSION

There are various sources of uncertainty inherent in the data being used to perform this analysis. For example, we have not taken the stellar limb-darkening into account when considering transit durations. However, in all cases we only consider the total duration (first contact to last contact) and so this will be a negligible effect. For the Kepler candidates, the primary source of uncertainty arises from the stellar parameters which are used to derive many of the planetary candidate parameters. The prime culprit in this regard are the stellar radii which are difficult to determine to within 10% even when spectra are available. Our assumption however is that these uncertainties are not significantly biased in one direction of the other and thus add noise to the overall statistical properties. One method to test this assumption is to consider multi-candidate systems for which a change in the stellar radius will effect all calculated transit durations in a similar way. For example, KOI 157 has 6 detected planet candidates with shorter than predicted measured transit durations and an estimated host star

radius of $1.06 R_{\odot}$. Reducing the stellar radius slightly makes 2 of the planets consistent with a circular orbit but leaves the other durations as highly discrepant. A more global approach is to attempt to create a systematic dependence in the stellar radii that would produce transit durations consistent with circular orbits for the bulk of the distribution. This also failed to change the mean of the distribution resulting in the conclusion that the distribution is not due to systematically incorrect stellar radii.

For the radial velocity stars, we have attempted to retain only the main sequence stars in our sample but the stellar radii are likewise prone to similar uncertainties. As such, our limits on the eccentricities of the specific Kepler candidates discussed in Section 4 should be treated in the context of these uncertainties and indeed we concentrate our comments on the global distribution of all the Kepler objects and their parameters. Note also that the Kepler sample is only complete to ~ 0.5 AU with declining completeness beyond this to ~ 1.5 AU. Thus the number of candidates beyond 0.5 AU are smaller but still sufficient for a valid comparison to be made.

One aspect of the Kepler candidates which was not taken into account was the multiplicity of the systems. As suggested at the conclusion of the previous section, the multiplicity may indeed play a significant role in stabilizing planets in approximately circular orbits, particularly for those in the low mass/size regime. This is true of the radial velocity planets also, some of which are known to lie in multiple systems of super-Earth mass planets and with relatively circular orbits such as the system orbiting HD 10180 (Lovis et al. 2011).

A minor impact on the stellar radii that should be noted is that due to the planet-metallicity correlation. Johnson et al. (2010) explored the mass-metallicity relationship for star that harbor planets and found a significant positive correlation of planet frequency with both stellar mass and metallicity, in concordance with the findings of Fischer & Valenti (2005). For a given stellar mass, a larger metallicity leads to a smaller radius

in order to reach hydrostatic equilibrium. The implication for this study is that many of the Kepler host stars will have relatively high metallicity leading to an over-estimated radius. However, this effect is at the level of a few percent and not expected to interfere with the results of this study.

7. CONCLUSIONS

By conducting a transit survey which is sensitive to long enough periods, it is expected that one will eventually reproduce the eccentricity distribution found amongst radial velocity planets, however this hasn't been possible until the Kepler mission has allowed such a large sample of long-period planets to be detected. For individual planets, the eccentricity may be discerned through an asymmetry in the shape of ingress and egress (Kipping 2008). This requires exquisite photometry and is highly sensitive to the orbital orientation (periastron argument) of the orbit. We have shown here that the new release of Kepler candidates provides both the numbers and period range needed in order to assess their agreement with the radial velocity planets and that a consistent model of the eccentricity distribution is reached. The correlation of eccentricity with planet size is also an expected result based upon the discoveries of small planets in multiple systems and indicates that there is an empirical approach from which to both reverse-engineer formation scenarios and predict future stability patterns.

ACKNOWLEDGEMENTS

The authors would like to thank Andrew Howard for several useful discussions. This research has made use of the Exoplanet Orbit Database and the Exoplanet Data Explorer at exoplanets.org. This research has also made use of the NASA Exoplanet Archive, which is operated by the California Institute of Technology, under contract with the National Aeronautics and Space Administration under the Exoplanet Exploration Program.

REFERENCES

- Batalha, N.M., et al., 2012, ApJS, submitted (arXiv:1202.5852)
 Borucki, W.J., et al., 2011, ApJ, 728, 117
 Borucki, W.J., et al., 2011, ApJ, 736, 19
 Butler, R.P., et al., 2006, ApJ, 646, 505
 Burke, C.J., 2008, ApJ, 679, 1566
 Fischer, D.A., Valenti, J., 2005, ApJ, 622, 1102
 Ford, E.B., Quinn, S.N., Veras, D., 2008, ApJ, 678, 1407
 Ford, E.B., Rasio, F.A., 2008, ApJ, 686, 621
 Goldreich, P., Soter, S., 1966, Icarus, 5, 375
 Howard, A.W., et al., 2010, Science, 330, 653
 Johnson, J.A., Aller, K.M., Howard, A.W., Crepp, J.R., 2010, PASP, 122, 905
 Jurić, M., Tremaine, S., 2008, ApJ, 686, 603
 Kane, S.R., Gelino, D.M., 2012, PASP, in press (arXiv:1202.2377)
 Kane, S.R., von Braun, K., 2008, ApJ, 689, 492
 Kane, S.R., von Braun, K., 2009, PASP, 121, 1096
 Kipping, D.M., 2008, MNRAS, 389, 1383
 Lissauer, J.J., et al., 2011, ApJS, 197, 8
 Lissauer, J.J., et al., 2011, ApJ, in press (arXiv:1201.5424)
 Lovis, C., et al., 2011, A&A, 528, 112
 Malmberg, D., Davies, M.B., 2009, MNRAS, 394, L26
 Mandel, K., Agol, E., 2002, ApJ, 580, L171
 Matsumura, S., Takeda, G., Rasio, F.A., 2008, ApJ, 686, L29
 Pont, F., Husnood, N., Mazeh, T., Fabrycky, D., 2011, MNRAS, 414, 1278
 Seager, S., Mallén-Ornelas, G., 2003, ApJ, 585, 1038
 Shen, Y., Turner, E.L., 2008, ApJ, 685, 553
 Smalley, B., 2005, Mem. Soc. Astron. Ital. Suppl., 8, 130
 von Braun, K., Kane, S.R., Ciardi, D.R., 2009, ApJ, 702, 779
 Wang, J., Ford, E.B., 2011, MNRAS, 418, 1822
 Wright, J.T., et al., 2011, PASP, 123, 412
 Zakamska, N.L., Pan, M., Ford, E.B., 2011, MNRAS, 410, 1895